23. Gafter-Gvili A, Fraser A, Paul M, Leibovici L. Meta-analysis: antibiotic prophylaxis reduces mortality in neutropenic patients. Ann Intern Med 2005; 142 (12, Part 1): 979–995.
24. Radice C, Munoz V, Castellares C, et al. *Listeria monocytogenes* meningitis in two allogeneic hematopoietic stem cell transplant recipients. Leuk Lymphoma 2006; 47 (8): 1701–1703.
25. Sullivan KM, Dykewicz CA, Longworth DL, et al. Preventing opportunistic infections after hematopoietic stem cell transplantation: the Centers for Disease Control and Prevention, Infectious Diseases Society of America, and American Society for Blood and Marrow Transplantation Practice Guidelines and beyond. Hematology Am Soc Hematol Educ Program 2001; 392–421.
26. Bilgrami S, Aslanzadeh J, Feingold JM, et al. Cytomegalovirus viremia, viruria and disease after autologous peripheral blood stem cell transplantation: no need for surveillance. Bone Marrow Transplant 1999; 24: 69–73.
27. Nagafuji K, Eto T, Hayashi S, Tokunaga Y, Gondo H, Niho Y. Fatal cytomegalovirus interstitial pneumonia following autologous peripheral blood stem cell transplantation. Fukuoka Bone Marrow Transplantation Group. Bone Marrow Transplant 1998; 21 (3): 301–303.
28. Frere P, Pereira M, Fillet G, Beguin Y. Infections after CD34-selected or unmanipulated autologous hematopoietic stem cell transplantation. Eur J Haematol 2006; 76 (2): 102–108.
29. La Rosa AM, Champlin RE, Mirza N, et al. Adenovirus infections in adult recipients of blood and marrow transplants. Clin Infect Dis 2001; 32 (6): 871–876.
30. Chakrabarti S, Mautner V, Osman H, et al. Adenovirus infections following allogeneic stem cell transplantation: incidence and outcome in relation to graft manipulation, immunosuppression, and immune recovery. Blood 2002; 100 (5): 1619–1627.
31. Symeonidis N, Jakubowski A, Pierre-Louis S, et al. Invasive adenoviral infections in T-cell-depleted allogeneic hematopoietic stem cell transplantation: high mortality in the era of cidofovir. Transpl Infect Dis 2007; 9 (2): 108–113.
32. Takeshima M, Takamatsu H, Iida M, Mochizuki Y, Okumura H, Yoshida T. Frequent viral infections and delayed CD4 + cell recovery following CD34 + cell-selected autologous peripheral blood stem cell transplantation. Int J Hematol 1999; 70 (3): 193–199.
33. Moore J, Brooks P, Milliken S, et al. A pilot randomized trial comparing CD34-selected versus unmanipulated hemopoietic stem cell transplantation for severe, refractory rheumatoid arthritis. Arthritis Rheum 2002; 46 (9): 2301–2309.
34. Kanda Y, Mineishi S, Saito T, et al. Long-term low-dose acyclovir against varicella-zoster virus reactivation after allogeneic hematopoietic stem cell transplantation. Bone Marrow Transplant 2001; 28 (7): 689–692.
35. Asano-Mori Y, Kanda Y, Oshima K, et al. Long-term ultra-low-dose acyclovir against varicella-zoster virus reactivation after allogeneic hematopoietic stem cell transplantation. Am J Hematol 2008; 83 (6): 472–476.

INTERNAL MEDICINE

□ CASE REPORT □

Encephalomyelitis Mimicking Multiple Sclerosis Associated with Chronic Graft-Versus-Host Disease after Allogeneic Bone Marrow Transplantation

Yayoi Matsuo[1], Kenjiro Kamezaki[1], Shoichiro Takeishi[1], Katsuto Takenaka[1], Tetsuya Eto[2], Atsushi Nonami[1], Toshihiro Miyamoto[1], Hiromi Iwasaki[3], Naoki Harada[1], Koji Nagafuji[1], Takanori Teshima[3] and Koichi Akashi[1]

Abstract

We describe a case of encephalomyelitis mimicking multiple sclerosis associated with chronic graft-versus-host disease (GVHD) occurring after allogeneic bone marrow transplanation (BMT) for myelodysplastic syndrome. Immunosuppressive therapy, consisting of a therapeutic dose of cyclosporine A and a maintenance dose of methylprednisolone, was effective in treating symptoms. Although central nervous system GVHD is very rare and remains controversial, presentation of neurological symptoms after allogeneic BMT warrants consideration of GVHD in the differential diagnosis.

Key words: allogeneic bone marrow transplantation, graft-versus-host disease, multiple sclerosis

(Inter Med 48: 1453-1456, 2009)
(DOI: 10.2169/internalmedicine.48.2003)

Introduction

Bone marrow transplantation (BMT) recipients are at high risk for neurological complications, including infection, metabolic abnormalities, drug toxicity, cerebrovascular events, posterior reversible encephalopathy syndrome (PRES), Epstein-Barr virus-associated lymphoproliferative disease (EBV-LPD), and relapse of malignant disease in the central nervous system (CNS) (1). Graft-versus-host disease (GVHD) is a systemic complication after BMT mediated by donor T cells targeting the skin, gastrointestinal tract, and liver. Involvement of other organ systems has been observed, but effects on the CNS are rare and controversial (2). Here, we describe a case of immune-mediated encepalomyelopathy mimicking MS associated with chronic GVHD after allogeneic BMT.

Case Report

In 1996, a 22-year-old woman was diagnosed with myelodysplastic syndrome (MDS). In 2006, she became transfusion-dependent and underwent allogeneic BMT using donor cells from her HLA-identical brother in May 2006. Transplant conditioning and GVHD prophylaxis consisted of busulfan (4 mg/kg per day for 4 days) plus cyclophosphamide (60 mg/kg per day for 2 days) and cyclosporin A (CyA) plus short methotrexate, respectively. Rapid engraftment and sustained complete donor chimerism was achieved. Her transplant course was uneventful and no acute GVHD was observed until two months after transplantation. CyA was tapered off and discontinued five months after transplantation.

Six months after transplantation, the patient developed pancytopenia, liver dysfunction, and oral lichen planus (Fig. 1). Her bone marrow cells showed no dysplasia of trilineage blood cells, and complete donor chimerism of bone

[1]Medicine and Biosystemic Science, Kyushu University Graduate School of Medical Sciences, Fukuoka, [2]Department of Hematology, Hamanomachi General Hospital, Fukuoka and [3]Center for Cellular and Molecular Medicine, Kyushu University Hospital, Fukuoka
Received for publication December 31, 2008; Accepted for publication May 7, 2009
Correspondence to Dr. Kenjiro Kamezaki, kamezaki@pa2.so-net.ne.jp

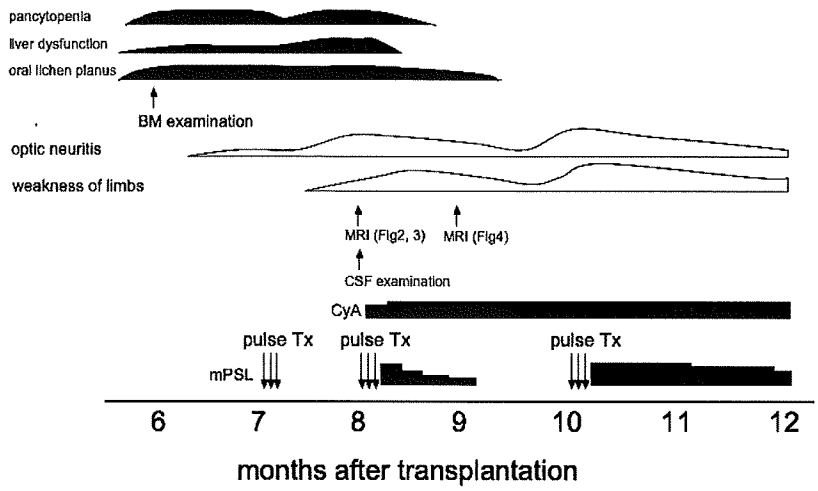

Figure 1. Clinical course of the patient. BM: bone marrow, MRI: magnetic resonance imaging, CSF: cerebrospinal fluid, CyA: cyclosporine A, Tx: therapy, mPSL: methylprednisolone

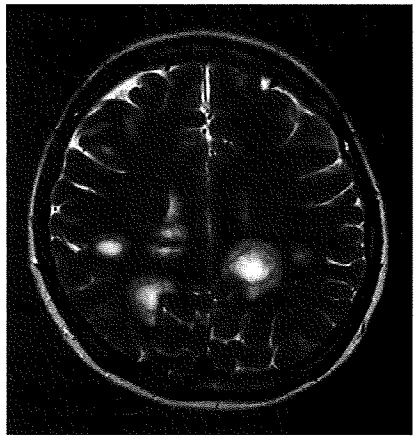

Figure 2. T2-weighted MRI of the brain reveals multiple white matter lesions.

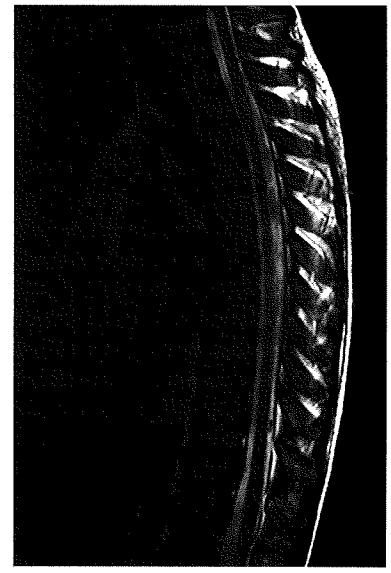

Figure 3. Spinal MRI reveals a high intensity lesion of the thoracic spinal cord.

marrow cells was maintained, as determined by variable number of tandem repeat analysis. At this time, she was diagnosed with chronic GVHD.

Seven months after transplantation, the patient developed blurred vision in the right eye and was diagnosed with optic neuritis after fundus examination revealed optic nerve head edema (Fig. 1). However, brain magnetic resonance imaging (MRI) did not reveal white matter lesions or optic nerve abnormalities at that time. She received methylprednisolone pulse therapy (1 g/day for 3 days), but her visual acuity gradually worsened. In addition, she gradually developed weakness and numbness of the lower limbs, urinary retention, and blurred vision in both eyes. Her visual acuity declined rapidly, finally becoming only able to observe counting fingers. Brain and spinal MRI revealed multiple high intensity lesions of white matter mainly in the right posterior limb of the internal capsule and thalamus (Fig. 2) and in the thoracic spine (Fig. 3). These lesions were enhanced with gadolinium. Cerebrospinal fruid (CSF) was clear, with normal pressure, cell counts (3 cells/μL), and myelin basic protein levels, glucose at 64 mg/dL, total protein at 20.0 mg/dL, IgG at 1.32 mg/dL, and an IgG index of 0.50. Oligoclonal bands were not detected in the CSF sample. Cytology of CSF revealed no evidence of malignancy and cultures of CSF were negative for bacteria and fungus. CSF for CMV, HHV-6, EBV, JC virus, and toxoplasma were negative for polymerase chain reaction (PCR).

The patient was subsequently treated with CyA and methylprednisolone pulse therapy. Neurological symptoms and white matter lesions visible by MRI improved (Fig. 4). Other manifestations of chronic GVHD also achieved remission. However, she developed weakness and numbness of

Figure 4. MRI of the brain after immunosuppressive therapy shows improvement of white matter lesions.

the upper and lower limbs again after methylprednisolone was tapered off, even though a therapeutic dose of CyA was administered at that time. Spinal MRI revealed new lesions of the cervical spine. The patient was again treated with methylprednisolone pulse therapy, and her neurological symptoms and radiological lesions of the cervical spine improved (Fig. 1). Improved neurological symptoms remained stable two years after transplantation, despite tapering of the methylprednisolone dose to 0.5 mg/kg.

Discussion

Although GVHD commonly affects the skin, gastrointestinal tract, liver, and hematopoietic system, recent reports have described patients with neurologic manifestations associated with GVHD (2-14). Animal studies support the possibility of the brain being a target organ for GVHD (15), however, CNS-GVHD remains controversial. CNS-GVHD may be properly diagnosed only if there is no evidence of other diseases with overlapping features and if radiographic characteristics of CNS involvement, response to immunosuppressive therapy, and T cell infiltration according to histological evaluation are observed (2). In the present case, negative evaluation for infection, multiple radiological lesions of the brain and spinal white matter, the development of systemic GVHD after discontinuation of CyA, and a response to CyA plus methylprednisolone immunosuppressive therapy support a diagnosis of CNS-GVHD, even though we do not have histological data.

Our patient developed optic neuritis and myelitis in separate time courses. MRI imaging revealed multiple white matter lesions of the brain and spinal cord. Acute disseminated encephalomyelitis (ADEM) also shows such multiple white matter lesions and typically follows an acute monophasic clinical course (16). These separate episodes of neurologic symptoms and radiological findings are characteristic of MS, which is thought to be caused by immune-mediated demyelination. Immune-mediated myelitis after BMT is very rare, with only three other reported cases in the English literature (8, 11, 13).

There is no consensus on treatment options for CNS-GVHD. In most cases previously reported in the literature, treatment consisted of high-dose methylprednisolone or calcineurin-inhibitor (2). The present patient was first treated with methylprednisolone alone for optic neuritis, but her visual acuity worsened and neurological symptoms caused by myelitis emerged. After treatment with CyA plus methylprednisolone as a second line therapy for chronic GVHD (17), the neurological deficits improved. The patient developed myelitis again after methylprednisolone was discontinued. Finally, after treatment with CyA plus a maintenance dose of methylprednisolone, the neurological symptoms stabilized. This clinical course may indicate that as with systemic GVHD in other organs, a therapeutic dose of calcineurin inhibitor and a maintenance dose of corticosteroid for second line therapy are necessary for the treatment of CNS-GVHD.

Clinically significant CNS-GVHD is rare, but the consequences can be serious. A diagnosis of CNS-GVHD should be considered in cases of neurologic symptoms after allogeneic BMT if there is no evidence of other diseases with overlapping features and if radiographic characteristics of CNS involvement and response to immunosuppressive therapy are observed.

References

1. Siegal D, Keller A, Xu W, et al. Central nervous system complications after allogeneic hematopoietic stem cell transplantation: incidence, manifestations, and clinical significance. Biol Blood Marrow Transplant **13**: 1369-1379, 2007.
2. Kamble RT, Chang CC, Sanchez S, Carrum G. Central nervous system graft-versus-host disease: report of two cases and literature review. Bone Marrow Transplant **39**: 49-52, 2007.
3. Campbell JN, Morris PP. Cerebral vasculitis in graft-versus-host disease: a case report. AJNR Am J Neuroradiol **26**: 654-656, 2005.
4. Iwasaki Y, Sako K, Ohara Y, et al. Subacute panencephalitis associated with chronic graft-versus-host disease. Acta Neuropathol **85**: 566-572, 1993.
5. Ma M, Barnes G, Pulliam J, et al. CNS angiitis in graft vs host disease. Neurology **59**: 1994-1997, 2002.
6. Marosi C, Budka H, Grimm G, et al. Fatal encephalitis in a patient with chronic graft-versus-host disease. Bone Marrow Transplant **6**: 53-57, 1990.
7. Nagashima T, Sato F, Chuma T, et al. Chronic demyelinating polyneuropathy in graft-versus-host disease following allogeneic bone marrow transplantation. Neuropathology **22**: 1-8, 2002.
8. Openshaw H, Slatkin NE, Parker PM, Forman SJ. Immune-mediated myelopathy after allogeneic marrow transplantation. Bone Marrow Transplant **15**: 633-636, 1995.
9. Padovan CS, Bise K, Hahn J, et al. Angiitis of the central nervous system after allogeneic bone marrow transplantation? Stroke **30**: 1651-1656, 1999.
10. Provenzale JM, Graham ML. Reversible leukoencephalopathy as-

sociated with graft-versus-host disease: MR findings. AJNR Am J Neuroradiol **17**: 1290-1294, 1996.

11. Sakai M, Ohashi K, Ohta K, et al. Immune-mediated myelopathy following allogeneic stem cell transplantation. Int J Hematol **84**: 272-275, 2006.

12. Shortt J, Hutton E, Faragher M, Spencer A. Central nervous system graft-versus-host disease post allogeneic stem cell transplant. Br J Haematol **132**: 245-247, 2006.

13. Solaro C, Murialdo A, Giunti D, Mancardi G, Uccelli A. Central and peripheral nervous system complications following allogeneic bone marrow transplantation. Eur J Neurol **8**: 77-80, 2001.

14. Takatsuka H, Okamoto T, Yamada S, et al. New imaging findings in a patient with central nervous system dysfunction after bone marrow transplantation. Acta Haematol **103**: 203-205, 2000.

15. Hickey WF, Kimura H. Graft-vs.-host disease elicits expression of class I and class II histocompatibility antigens and the presence of scattered T lymphocytes in rat central nervous system. Proc Natl Acad Sci USA **84**: 2082-2086, 1987.

16. Tomonari A, Tojo A, Adachi D, et al. Acute disseminated encephalomyelitis (ADEM) after allogeneic bone marrow transplantation for acute myeloid leukemia. Ann Hematol **82**: 37-40, 2003.

17. Higman MA, Vogelsang GB. Chronic graft versus host disease. Br J Haematol **125**: 435-454, 2004.

Int J Hematol (2010) 91:107–111
DOI 10.1007/s12185-009-0453-8

CASE REPORT

Successful treatment of refractory advanced nasal NK/T cell lymphoma with unrelated cord blood stem cell transplantation incorporating focal irradiation

Yasuo Mori · Takatoshi Aoki · Katsuto Takenaka · Takuji Yamauchi · Asataro Yamamoto · Kenjiro Kamezaki · Hiromi Iwasaki · Naoki Harada · Toshihiro Miyamoto · Koji Nagafuji · Takanori Teshima · Koichi Akashi

Received: 2 September 2009 / Revised: 7 November 2009 / Accepted: 13 November 2009 / Published online: 2 December 2009

Abstract Nasal natural killer (NK)/T cell lymphoma is a rare disease with a poor prognosis. We report the case of a 52-year-old woman with progressive advanced nasal NK/T cell lymphoma, with local invasiveness and bone marrow involvement, who was successfully treated with unrelated cord blood transplantation (UCBT). The patient was initially refractory to conventional chemotherapy. She was therefore treated with local irradiation, which induced a partial response. The patient then underwent UCBT using a conditioning regimen consisting of cyclophosphamide and total body irradiation. Acute graft-versus-host disease involving the skin was observed, but it was well controlled without systemic administration of corticosteroids. The patient remained in complete remission for 18 months after UCBT. Although the observation period has been relatively short and longer follow-up is needed, our observations suggest that incorporating focal irradiation to conditioning regimen for local control might be an effective treatment option for advanced nasal NK/T cell lymphoma in the setting of UCBT.

Y. Mori (✉) · T. Aoki · K. Takenaka · T. Yamauchi · A. Yamamoto · K. Kamezaki · N. Harada · T. Miyamoto · K. Nagafuji · K. Akashi
Medicine and Biosystemic Science, Kyushu University Graduate School of Medical Sciences, 3-1-1 Maidashi, Higashi-ku, Fukuoka 812-8582, Japan
e-mail: velcade@intmed1.med.kyushu-u.ac.jp

H. Iwasaki · T. Teshima · K. Akashi
Center for Cellular and Molecular Medicine, Kyushu University Hospital, Fukuoka, Japan

K. Nagafuji
Division of Hematology, Department of Medicine, Kurume University School of Medicine, Fukuoka, Japan

Keywords Cord blood transplant · NK/T cell lymphoma · Refractory disease · Focal irradiation

1 Introduction

Natural killer (NK)/T cell lymphoma is currently been recognized to be a distinct clinical entity [1–3]. Most cases of NK/T cell lymphoma occur in the nasal or nasopharyngeal region and are often characterized by progressive, destructive ulceration and necrotic granulation. Nasal NK/T cell lymphomas are more common in Asian countries than in Western countries [2, 4]. Localized disease has a relatively good prognosis after combination therapy that includes anticancer drug and field radiation. However, advanced NK/T cell lymphoma is invariably fatal despite treatment with various chemotherapies or radiotherapy [5–8].

A few studies showed that high-dose chemotherapy with autologous or allogeneic stem cell rescue improved outcomes in selected cases [9–16]. However, because of the rarity of advanced nasal NK/T cell lymphoma, there is no general consensus concerning its optimal management. Recently, an alternative stem cell source has been used to treat some patients without available human leukocyte antigen (HLA)-matched donors. We herein report a rare case with disseminated nasal NK cell lymphoma that was successfully treated with unrelated cord blood transplantation (UCBT) incorporating focal irradiation during the refractory phase of the disease.

2 Case report

A 52-year-old woman consulted previous hospital because of left nasal obstruction, fever, and weight loss in October

2007. Physical examination revealed masses in the left nasal cavities. No peripheral lymphadenopathy was detected. The results of complete blood count and coagulation studies were normal. The lactate dehydrogenase concentration was 203 IU/l (normal range 119–229 IU/l), and the soluble interleukin-2 receptor concentration was slightly elevated to 592 U/ml (normal range < 466 U/ml). The results of serological tests for Epstein–Barr virus (EBV) antibodies were as follows: EBV viral capsid antigen (VCA), IgG 1:160, IgM < 1:10, and EB nuclear antigens (EBNA), 1:40. The EBV DNA load measured by quantitative polymerase chain reaction was not tested. Computed tomography (CT) and magnetic resonance imaging (MRI) revealed that the left nasal cavities were filled and the paranasal cavities were partially infiltrated with a tumor (Fig. 1a). ^{18}F-Fluorodeoxyglucose positron emission tomography revealed nasal cavity uptake and involvement of the bone marrow and spleen. Biopsy of the nasal tumor showed infiltration with medium to large-sized abnormal lymphoid cells involving necrotic tissues. Immunohistochemical examination showed the cells to be positive for CD56 and CD45RO (UCHL-1), and negative

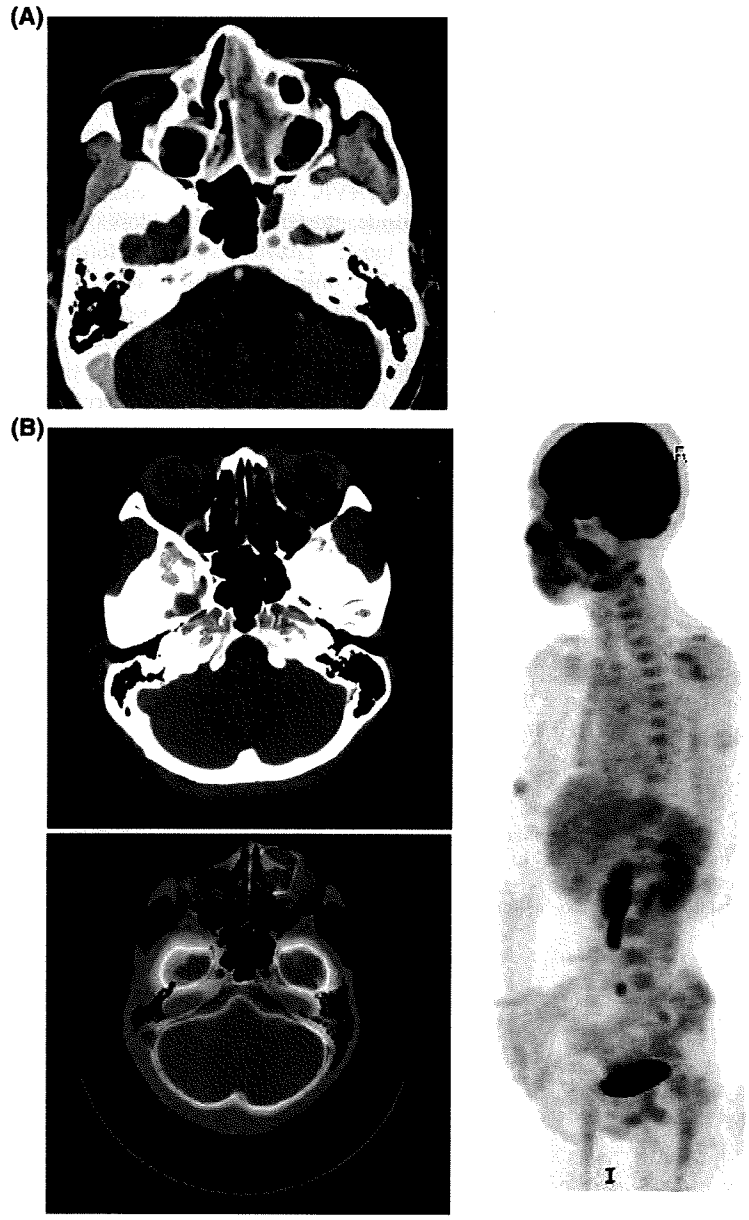

Fig. 1 **a** Left nasal cavity was occupied with NK/T cell lymphoma at the time of diagnosis. **b** MR and PET/CT findings before transplantation. Nasal tumor progressed with local invasion

for surface CD3. Using in situ hybridization, the presence of EBV-encoded small nuclear early region RNA was detected in the tumor tissues. Bone marrow aspiration revealed involvement of abnormal lymphoma cells in 4.4% of the nucleated cells. On the basis of these findings, a diagnosis of extranodal NK/T cell lymphoma, nasal type, was made in accordance with WHO guidelines. The clinical stage was determined to be Ann Arbor stage IVB.

The patient received an induction chemotherapy consisting of dexamethasone, methotrexate, ifosfamide, L-asparaginase, and etoposide [17]. Partial response was transiently achieved as the best response after 5 courses of chemotherapy, but the disease soon progressed. Because the prognosis of advanced nasal NK/T cell lymphoma is extremely poor, the patient was referred to our hospital for allogeneic stem cell transplantation in April 2008. On admission, nasal obstruction and local tumor invasiveness were observed (Fig. 1b). To reduce the tumor burden before transplantation, we performed DeVIC chemotherapy consisting of carboplatin, etoposide, ifosfamide, and dexamethasone. However, nasal tumor growth was observed soon after this treatment. The disease was so aggressive that we planned an allogeneic transplantation using cord blood as an alternative stem cell source, because the patient had no HLA-identical sibling donor and there is little time to find a suitable donor from Japan marrow donor bank. For local control of the tumor before UCBT, the patient was scheduled to receive additional 10 Gy nasal irradiation before preparative regimen that was considered as tolerable and maximum dose we could add before the conditioning, because the disease was refractory to chemotherapy. To maximize the efficacy and minimize the adverse effect for subsequent conventional conditioning regimen, we decided to perform 5 fractioned local irradiation until 2 days before the administration of cyclophosphamide (10 Gy in 5 fractions on day−12 to −8). The patient then received a conventional conditioning regimen consisting of cyclophosphamide (60 mg/kg on days −6 to −5), and total body irradiation (12 Gy in 6 fractions on days −3 to −1). UCBT was performed on May 2008. The numbers of infused cells and CD34 positive cells were 4.7×10^7/kg and 1.66×10^5/kg, respectively. The patient and donor were one-antigen mismatched as determined by serological and DNA typing. Graft-versus-host disease (GVHD) prophylaxis consisted of intravenous cyclosporin (3 mg/kg/day) beginning on day −1 and short-term methotrexate on days 1 (10 mg/m^2), 3 (7 mg/m^2), and 6 (7 mg/m^2). Granulocyte colony-stimulating factor was administered from days 1 to 26 to accelerate neutrophil recovery. Rapid engraftment was obtained. A neutrophil count > 500/μl, a platelet count > 50,000/μl, and a reticulocyte count > 20,000/μl were achieved on days 17, 32, and 21, respectively, and complete donor chimerism was observed in a bone marrow sample on day 28. The patient tolerated the preparative regimen well, and regimen-related toxicity consisted of only febrile neutropenia (Grade 3) and appetite loss (Grade 3), both of which were self-limiting. An MRI performed 18 days after the allogeneic transplantation showed that the residual mass in the left nasal cavity and cervical lymph nodes had disappeared (Fig. 2a); thus, we concluded that the patient achieved a complete remission. Acute GVHD of the skin, confirmed by skin biopsy, was observed on day 21, and gradually progressed to Stage 3. Because no other sites (liver, gut) were involved, the patient was treated only with a topical corticosteroid and the symptoms resolved without the need for additional immunosuppressive agents. Cytomegalovirus antigenemia became positive on day 39 and was treated with 10 mg/kg/day gancyclovir. The patient was discharged from our hospital on day 66. Despite having extensive chronic GVHD (dry skin and pericardial effusion), the patient was still in complete remission (Fig. 2b) at the 18-month follow-up and was in excellent health otherwise.

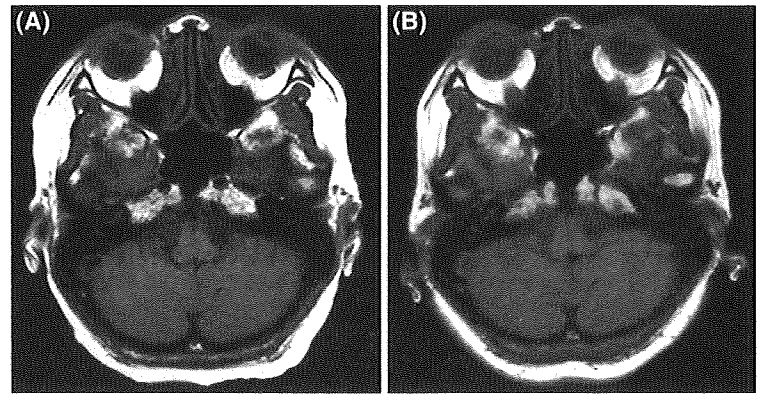

Fig. 2 MR scanning performed 18 days (**a**) and 6 months (**b**) after transplantation. She remained in complete remission

3 Discussion

Lymphoma of the NK/T cell phenotype is rare and nasal NK/T cell lymphoma, the most frequent disease in this category, accounts for only 1.85% of all malignant lymphomas in Japan [18]. Recently, the long-term outcomes and prognostic factors of patients with this rare disease have been elucidated. Localized nasal disease can be controlled with radiotherapy, but durable remission is achieved in only about 50% of patients, because dissemination occurs in most of these patients [5, 8]. Systemic dissemination is usually fatal. Cheung et al. [7] reported that all patients with advanced NK cell lymphoma treated with conventional chemotherapy died within 1 year of diagnosis.

In an effort to improve the survival rate, the efficacy of high-dose chemotherapy following autologous hematopoietic stem cell transplantation (auto-HSCT) has been studied; however, this strategy was only beneficial in patients with stage III or IV advanced NK/T cell lymphoma in complete remission and with high NK-IPI scores [13, 14]. In contrast, patients not in remission at the time of transplantation had significantly shorter relapse-free survival and poorer overall survival rates. Allogeneic HSCT (allo-HSCT) has been attempted in patients with advanced stage disease or with disease refractory to conventional chemotherapy. Murashige et al. [19] reported the retrospective analysis of 28 patients who underwent allo-HSCT. Although 19 of the 28 patients had active stage IV disease before allo-HSCT, 34% achieved long-term progression-free survival. Notably, all of the patients who did not relapse or progress within 10 months remained free of progression. Suzuki et al. [20] evaluated the effects of allo-HSCT in 15 patients with NK-cell lineage neoplasms. The probability of relapse was as low as 17%, even though 60% of the patients underwent transplantation during remission failure. These data suggest the presence of a graft-versus-lymphoma (GVL) effect, which plays an important role in disease eradication. However, in most reported cases, bone marrow or peripheral blood from sibling donors or HLA-matched unrelated donors was used as the stem cell source. Recently, the use of HSCT with UCB has increased in patients with no suitable donor, and its safety and efficacy have been gradually established. Only one case of nasal NK/T cell lymphoma treated with UCBT has been reported previously [21]. A 36-year-old woman in second complete remission underwent UCBT after a preparative regimen, consisting of total body irradiation, cyclophosphamide, and cytarabine. She remained in remission for 33 months after transplantation with self-limiting acute GVHD. In contrast, our case achieved complete remission after undergoing UCBT for progressive disease. Additional focal irradiation might play an important role for eradicating the residual mass and inhibiting early recurrence. Generally, NK/T cell lymphoma has been recognized resistant to chemotherapy because of its expression of the multidrug-resistant p-glycoprotein but relatively sensitive to radiotherapy. At present, radiotherapy followed by chemotherapy [22] or simultaneous chemoradiotherapy (RT-DeVIC) are regarded as an optimal treatment strategy for limited stage of nasal NK/T cell lymphomas. Recent report has disclosed that only radiotherapy but not chemotherapy improved outcome of relapsed nasal NK/T cell lymphoma as salvage treatment [23]. On the other hand, for cases with advanced stages, chemotherapy using multiple anti-cancer drugs including L-asparaginase was usually selected and concurrent radiotherapy was omitted in initial treatment. Because local tumor invasiveness was reported to be an adverse prognostic factor [24], additional focal irradiation for local control might take advantage even in advanced cases. In our case, incorporating focal irradiation to preparative conditioning was partly responsible for achieving complete remission soon after subsequent UCBT, and following GVL effect could contribute to her relapse-free survival of 18 months. Incorporating focal RT to conventional preparative regimen may be expected better clinical course by reducing regimen-related toxicity and tumor burden before transplantation than additional administration of systemic anti-cancer drugs even in patients with advanced NK/T cell lymphoma. Further accumulation of data was required to assess the efficacy and the optimal dose or timing of radiotherapy for patients with advanced stages.

In conclusion, we reported a rare case with refractory advanced nasal NK/T cell lymphoma successfully treated with local irradiation following UCBT. UCB could be considered as alternative source of stem cells for NK/T cell lymphoma patients with no suitable donor even though the disease is in refractory phase.

References

1. Kanavaros P, et al. Nasal T-cell lymphoma: a clinicopathologic entity associated with peculiar phenotype and with Epstein-Barr virus. Blood. 1993;81(10):2688–95.
2. Jaffe ES, et al. Report of the workshop on nasal and related extranodal angiocentric T/natural killer cell lymphomas. Definitions, differential diagnosis, and epidemiology. Am J Surg Pathol. 1996;20(1):103–11.
3. Nakamura S, et al. Clinicopathologic study of nasal T/NK-cell lymphoma among the Japanese. Pathol Int. 1997;47(1):38–53.
4. Jaffe ES. Classification of natural killer (NK) cell and NK-like T-cell malignancies. Blood. 1996;87(4):1207–10.
5. Liang R, et al. Treatment outcome and prognostic factors for primary nasal lymphoma. J Clin Oncol. 1995;13(3):666–70.
6. Kwong YL, et al. CD56+ NK lymphomas: clinicopathological features and prognosis. Br J Haematol. 1997;97(4):821–9.

7. Cheung MM, et al. Primary non-Hodgkin's lymphoma of the nose and nasopharynx: clinical features, tumor immunophenotype, and treatment outcome in 113 patients. J Clin Oncol. 1998;16(1):70–7.
8. Kim GE, et al. Angiocentric lymphoma of the head and neck: patterns of systemic failure after radiation treatment. J Clin Oncol. 2000;18(1):54–63.
9. Liang R, et al. Autologous bone marrow transplantation for primary nasal T/NK cell lymphoma. Bone Marrow Transpl. 1997;19(1):91–3.
10. Nawa Y, et al. Successful treatment of advanced natural killer cell lymphoma with high-dose chemotherapy and syngeneic peripheral blood stem cell transplantation. Bone Marrow Transpl. 1999;23(12):1321–2.
11. Sasaki M, et al. Successful treatment of disseminated nasal NK/T-cell lymphoma using double autologous peripheral blood stem cell transplantation. Int J Hematol. 2000;71(1):75–8.
12. Takenaka K, et al. High-dose chemotherapy with hematopoietic stem cell transplantation is effective for nasal and nasal-type CD56+ natural killer cell lymphomas. Leuk Lymphoma. 2001;42(6):1297–303.
13. Kim HJ, et al. High-dose chemotherapy with autologous stem cell transplantation in extranodal NK/T-cell lymphoma: a retrospective comparison with non-transplantation cases. Bone Marrow Transpl. 2006;37(9):819–24.
14. Lee J, et al. Autologous hematopoietic stem cell transplantation in extranodal natural killer/T cell lymphoma: a multinational, multicenter, matched controlled study. Biol Blood Marrow Transpl. 2008;14(12):1356–64.
15. Makita M, et al. Successful treatment of progressive NK cell lymphoma with allogeneic peripheral stem cell transplantation followed by early cyclosporine tapering and donor leukocyte infusions. Int J Hematol. 2002;76(1):94–7.
16. Reimer P, et al. What is CD4+CD56+ malignancy and how should it be treated? Bone Marrow Transpl. 2003;32(7):637–46.
17. Yamaguchi M, et al. Phase I study of dexamethasone, methotrexate, ifosfamide, L-asparaginase, and etoposide (SMILE) chemotherapy for advanced-stage, relapsed or refractory extranodal natural killer (NK)/T-cell lymphoma and leukemia. Cancer Sci. 2008;99(5):1016–20.
18. Lymphoma Study Group of Japanese Pathologists. The world health organization classification of malignant lymphomas in japan: incidence of recently recognized entities. Pathol Int. 2000;50(9):696–702.
19. Murashige N, et al. Allogeneic haematopoietic stem cell transplantation as a promising treatment for natural killer-cell neoplasms. Br J Haematol. 2005;130(4):561–7.
20. Suzuki R, et al. Hematopoietic stem cell transplantation for natural killer-cell lineage neoplasms. Bone Marrow Transpl. 2006;37(4):425–31.
21. Yokoyama H, et al. Successful treatment of advanced extranodal NK/T cell lymphoma with unrelated cord blood transplantation. Tohoku J Exp Med. 2007;211(4):395–9.
22. Li YX, et al. Radiotherapy as primary treatment for stage IE and IIE nasal natural killer/T-cell lymphoma. J Clin Oncol. 2006;24(1):181–9.
23. Zhang XX, et al. Salvage treatment improved survival of patients with relapsed extranodal natural killer/t-cell lymphoma, nasal type. Int J Radiat Oncol Biol Phys. 2009;74(3):747–52.
24. Kim TM, et al. Local tumor invasiveness is more predictive of survival than International Prognostic Index in stage I(E)/II(E) extranodal NK/T-cell lymphoma, nasal type. Blood. 2005; 106(12):3785–90.

Plenary paper

HapMap scanning of novel human minor histocompatibility antigens

*Michi Kamei,[1,2] *Yasuhito Nannya,[3-5] Hiroki Torikai,[1] Takakazu Kawase,[1,6] Kenjiro Taura,[7] Yoshihiro Inamoto,[8] Taro Takahashi,[8] Makoto Yazaki,[9] Satoko Morishima,[1] Kunio Tsujimura,[10] Koichi Miyamura,[5,8] Tetsuya Ito,[2] Hajime Togari,[2] Stanley R. Riddell,[11] Yoshihisa Kodera,[5,8] Yasuo Morishima,[5,12] Toshitada Takahashi,[13] Kiyotaka Kuzushima,[1] †Seishi Ogawa,[4,5] and †Yoshiki Akatsuka[1,5]

[1]Division of Immunology, Aichi Cancer Center Research Institute, Nagoya, Japan; [2]Department of Pediatrics and Neonatology, Nagoya City University, Graduate School of Medical Science, Nagoya, Japan; [3]Department of Hematology/Oncology and [4]The 21st Century Center of Excellence (COE) Program, Graduate School of Medicine, University of Tokyo, Tokyo, Japan; [5]Core Research for Evolutional Science and Technology, Japan Science and Technology Agency, Saitama, Japan; [6]Division of Epidemiology and Prevention, Aichi Cancer Center Research Institute, Nagoya, Japan; [7]Department of Information and Communication Engineering, Graduate School of Information Science, University of Tokyo, Tokyo, Japan; [8]Department of Hematology, Japanese Red Cross Nagoya First Hospital, Nagoya, Japan; [9]Department of Pediatrics, Higashi Municipal Hospital of Nagoya, Nagoya, Japan; [10]Department of Infectious Diseases, Hamamatsu University School of Medicine, Hamamatsu, Japan; [11]Program in Immunology, Clinical Research Division, Fred Hutchinson Cancer Research Center, Seattle, WA; [12]Department of Hematology and Cell Therapy, Aichi Cancer Center Central Hospital, Nagoya, Japan; and [13]Aichi Comprehensive Health Science Center, Aichi Health Promotion Foundation, Chita-gun, Japan

Minor histocompatibility antigens (mHags) are molecular targets of alloimmunity associated with hematopoietic stem cell transplantation (HSCT) and involved in graft-versus-host disease, but they also have beneficial antitumor activity. mHags are typically defined by host SNPs that are not shared by the donor and are immunologically recognized by cytotoxic T cells isolated from post-HSCT patients. However, the number of molecularly identified mHags is still too small to allow prospective studies of their clinical importance in transplantation medicine, mostly due to the lack of an efficient method for isolation. Here we show that when combined with conventional immunologic assays, the large data set from the International HapMap Project can be directly used for genetic mapping of novel mHags. Based on the immunologically determined mHag status in HapMap panels, a target mHag locus can be uniquely mapped through whole genome association scanning taking advantage of the unprecedented resolution and power obtained with more than 3 000 000 markers. The feasibility of our approach could be supported by extensive simulations and further confirmed by actually isolating 2 novel mHags as well as 1 previously identified example. The HapMap data set represents an invaluable resource for investigating human variation, with obvious applications in genetic mapping of clinically relevant human traits. (Blood. 2009;113:5041-5048)

Introduction

The antitumor activity of allogeneic hematopoietic stem cell transplantation (HSCT), which is a curative treatment for many patients with hematologic malignancies, is mediated in part by immune responses that are elicited as a consequence of incompatibility in genetic polymorphisms between the donor and the recipient.[1,2] Analysis of patients treated for posttransplantation relapse with donor lymphocytes has shown tumor regression to be correlated with expansion of cytotoxic T lymphocytes (CTLs) specific for hematopoiesis-restricted minor histocompatibility antigens (mHags).[3,4] mHags are peptides, presented by major histocompatibility complex (MHC) molecules, derived from intracellular proteins that differ between donor and recipient due mostly to single nucleotide polymorphisms (SNPs) or copy number variations (CNVs).[1,2,5] Identification and characterization of mHags that are specifically expressed in hematopoietic but not in other normal tissues could contribute to graft-versus-leukemia/lymphoma (GVL) effects, while minimizing unfavorable graft-versus-host disease, one of the most serious complications of allo-HSCT.[1,2] Unfortunately, however, efforts to prospectively target mHags to invoke T cell–mediated selective GVL effects have been hampered by the scarcity of eligible mHags, largely due to the lack of efficient methods for mapping the relevant genetic loci. Several methods have been developed to identify mHags, including peptide elution from MHC,[6,7] cDNA expression cloning,[8,9] and linkage analysis.[3,10] We have recently reported a novel genetic method that combines whole genome association scanning with conventional chromium release cytotoxicity assays (CRAs). With this approach the genetic loci of the mHag gene recognized by a given CTL clone can be precisely identified using SNP array analysis of pooled DNA generated from immortalized lymphoblastoid cell lines (LCLs) that are immunophenotyped into $mHag^+$ and $mHag^-$ groups by CRA.[11] The mapping resolution has now been improved from several Mb for conventional linkage analysis to an average haplotype block size of less than 100 kb,[12] usually containing a handful of candidate genes. Nevertheless, it still requires laborious DNA pooling and scanning of SNP arrays with professional expertise for individual

Submitted July 29, 2008; accepted August 27, 2008. Prepublished online as *Blood* First Editon paper, September 22, 2008; DOI 10.1182/blood-2008-07-171678.

*M.K. and Y.N. are first coauthors and contributed equally to this work.

†S.O. and Y.A. are senior coauthors.

An Inside *Blood* analysis of this article appears at the front of this issue.

The online version of this article contains a data supplement.

The publication costs of this article were defrayed in part by page charge payment. Therefore, and solely to indicate this fact, this article is hereby marked "advertisement" in accordance with 18 USC section 1734.

CTLs.[11] To circumvent these drawbacks, we have sought to take advantage of publicly available HapMap resources. Here, we describe a powerful approach for rapidly identifying mHAg loci using a large genotyping data set and LCLs from the International HapMap Project for genome-wide association analysis.[13-15]

Methods

Cell lines and CTL clones

The HapMap LCL samples were purchased from the Coriell Institute (Camden, NJ). All LCLs were maintained in RPMI1640 supplemented with 10% fetal calf serum, 2 mM L-glutamine, and 1 mM sodium pyruvate. Because the recognition of a mHag requires presentation on a particular type of HLA molecule, the LCLs were stably transduced with a retroviral vector encoding the restriction HLA cDNA for a given CTL clone when necessary.[16]

CTL lines were generated from recipient peripheral blood mononuclear cells obtained after transplantation by stimulation with those harvested before HSCT after irradiation (33 Gy), and thereafter stimulated weekly in RPMI 1640 supplemented with 10% pooled human serum and 2 mM L-glutamine. Recombinant human inerleukin-2 was added on days 1 and 5 after the second and third stimulations. CTL clones were isolated by standard limiting dilution and expanded as previously described.[10,17] HLA restriction was determined by conventional CRAs against a panel of LCLs sharing HLA alleles with the CTLs. All clinical samples were collected based on a protocol approved by the Institutional Review Board Committee at Aichi Cancer Center and the University of Tokyoand after written informed consent was obtained in accordance with the Declaration of Helsinki.

Immunophenotyping of HapMap LCLs and high-density genome-wide scanning of mHag loci

Case ($mHag^+$) - control ($mHag^-$) LCL panels were generated by screening corresponding restriction HLA-transduced CHB and JPT HapMap LCL panels with each CTL clone using CRAs. Briefly, target cells were labeled with 0.1 mCi of ^{51}Cr for 2 hours, and 10^3 target cells per well were mixed with CTL at a predetermined E/T ratio in a standard 4-hour CRA. All assays were performed at least in duplicate. The percent specific lysis was calculated by ((Experimental cpm - Spontaneous cpm) / (Maximum cpm - Spontaneous cpm)) × 100. After normalization by dividing their percent specific lysis values by that of positive control LCL (typically recipient-derived LCL corresponding to individual CTL clones), the mHag status of each HapMap LCL was defined as positive, negative, or undetermined.

To identify mHag loci, we performed association tests for all the Phase II HapMap SNPs, by calculating χ^2 test statistics based on 2 × 2 contingency tables with regard to the mHag status as measured by CRA and the HapMap genotypes (presence or absence of a particular allele) at each locus. χ^2 were calculated for the 2 possible mHag alleles at each locus and the larger value was adopted for each SNP. While different test statistics may be used showing different performance, the χ^2 statistic is most convenient for the purpose of power estimation as described below. The maximum value of the χ^2 statistics was evaluated against the thresholds empirically calculated from 100 000 random permutations within a given LCL set. The program was written in C++ and will run on a unix clone. It will be freely distributed on request. Computation of the statistics was performed within several seconds on a Macintosh equipped with 2 × quadcore 3.2 GHz Zeon processors (Apple, Cupertino, CA), although 100 000 permutations took several hours on average.

Evaluation of the power of association tests using HapMap samples

The genotyping data of the Phase II HapMap[14] were obtained from the International HapMap Project website (http://www.hapmap.org/genotypes/latest_ncbi_build35), among which we used the nonredundant data sets (excluding SNPs on the Y chromosome) from 60 CEU (Utah residents with ancestry from northern and western Europe) parents, 60 YRI (Yoruba in Ibadan, Nigeria) parents, and the combined set of 45 JPT (Japanese in Tokyo, Japan) and 45 CHB (Han Chinese in Beijing, China) unrelated people. They contained 3 901 416 (2 624 947 polymorphic), 3 843 537 (295 293 polymorphic), and 3 933 720 (2 516 310 polymorphic) SNPs for CEU, YRI, and JPT + CHB, respectively.

To evaluate the power, we first assumed that the Phase II HapMap SNP set contains the target SNP of the relevant mHag or its complete proxies, and that the immunologic assays can completely discriminate i $mHag^+$ and j $mHag^-$ HapMap LCLs. Under this ideal condition, the test statistic, or χ^2, for these SNPs takes a definite value, $f(i,j) = i+j$, which was compared with the maximum χ^2 value, or its distribution, under the null hypothesis, that is, no SNPs within the Phase II HapMap set should be associated with the mHag locus. Unfortunately, the latter distribution cannot be calculated in an explicit analytical form but needs to be empirically determined based on HapMap data, because Phase II HapMap SNPs are mutually interdependent due to extensive linkage disequilibrium within human populations. For this purpose, we simulated 10 000 case-control panels by randomly choosing i $mHag^+$ and j $mHag^-$ HapMap LCLs for various combinations of (i,j) and calculated the maximum χ^2 values (χ^2_{max}) for each panel to identify those (i,j) combinations, in which $f(i,j)$ exceeds the upper 1 percentile point of the simulated 10 000 maximum values, $g(i,j)^{P=.01}$.

When proxies are not complete (ie, $r^2 < 1$), the expected values will be decayed by the factor of r^2, and further reduced due to the probabilities of false positive (f_P) and negative (f_N) assays, and expressed as $\hat{f}(i,j) = (i + j) \times f^2$ through an apparent r^2 (f^2) as provided in formula 1.[1] Under given probabilities of assay errors and maximum LD strength between markers and the mHag allele, we can expect to identify target mHag loci for those (i,j) sets that satisfy $\hat{f}(i,j) > g(i,j)^{P=.01}$.

Empirical estimation of distributions of r^2

The maximum r^2 value (r^2_{max}) between a given mHag allele and one or more Phase II HapMap SNPs was estimated based on the observed HapMap data set. Each Phase II HapMap SNP was assumed to represent a target mHag allele, and the (r^2_{max}) was calculated, taking into account all the Phase II HapMap SNPs less than 500 kb apart from the target SNP.

Confirmatory genotyping

Genotyping was carried out either by TaqMan MGB technology (Applied Biosystems, Foster City, CA) with primers and probes for HA-1 mHag according to the manufacturer's protocol using an ABI 7900HT with the aid of SDS version 2.2 software (Applied Biosystems) or by direct sequencing of amplified cDNA for the *SLC1A5* gene. cDNA was reverse transcribed from total RNA extracted from LCLs, and polymerase chain reaction (PCR) was conducted with cDNA with the corresponding primers. Amplified DNA samples were sequenced using BigDye Terminator version 3.1 (Applied Biosystems). The presence or absence (deletion) of the *UGT2B17* gene was confirmed by genomic PCR with 2 primer sets for exons 1 and 6 as described previously[18] using DNA isolated from LCLs of interest.

Epitope mapping

A series of deletion mutant cDNAs were designed and cloned into pcDNA3.1/V5-His TOPO plasmid (Invitrogen, Carlsbad, CA). Thereafter, 293T cells that had been transduced with restricting HLA class I cDNA for individual CTL clones were transfected with each of the deletion mutants and cocultured with the CTL clone overnight to induce interferon (IFN)-γ release, which was then evaluated by enzyme-linked immunosorbent assay (ELISA) as previously described.[9]

For *SLC1A5*, expression plasmids encoding full-length cDNA and the exon 1 of recipient and donor origin were first constructed because only the SNP in the exon 1 was found to be concordant with susceptibility to CTL-3B6. Next, amino (N)- and (carboxyl) C-terminus–truncated mini-genes encoding polypeptides around the polymorphic amino acid defined by the SNP were amplified by PCR from *SLC1A5* exon 1 cDNA as template and cloned into the above plasmid. The constructs all encoded a Kozak

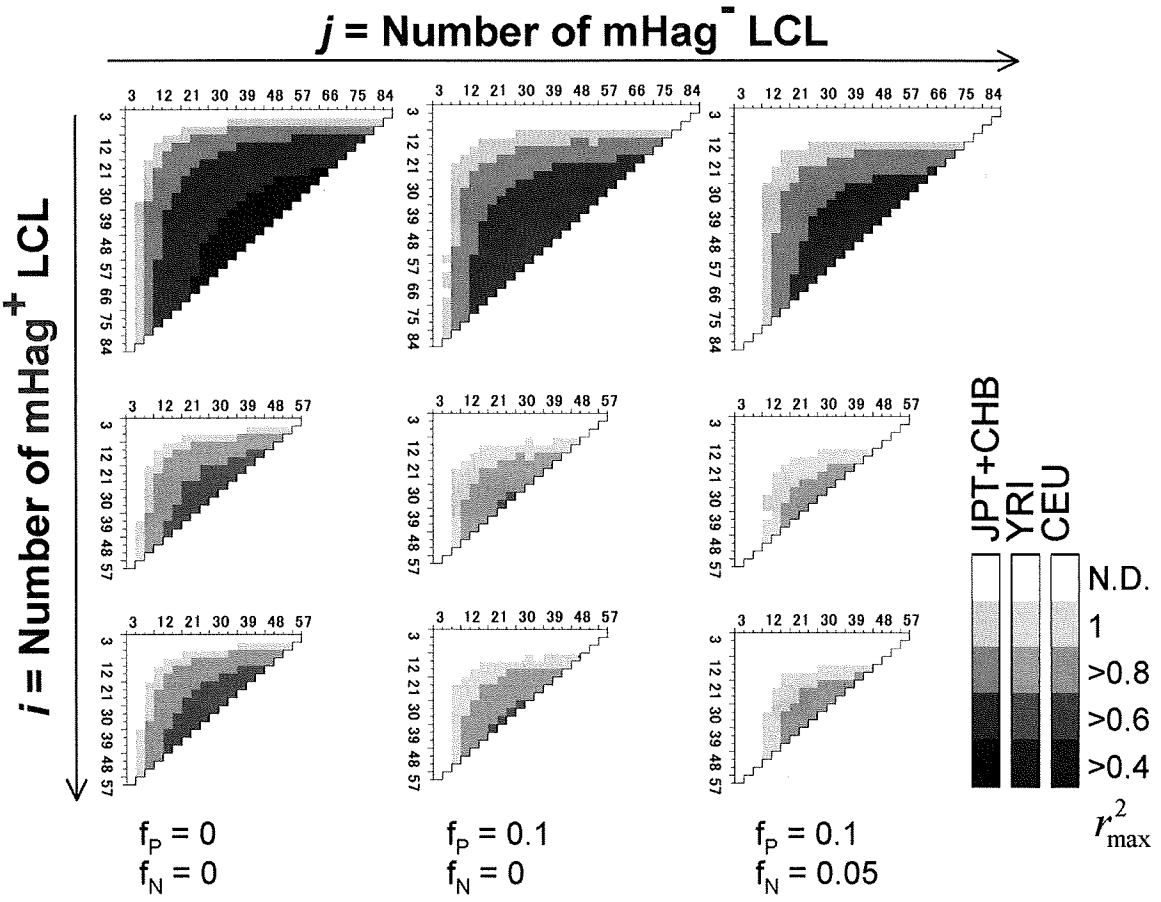

Figure 1. Numbers of positive and negative LCLs required for successful mHag mapping. The target locus was assumed to be uniquely identified, if the expected χ^2 value for the target SNP ($\hat{\chi}(i,j)$, see Document S1) exceeded the upper 1 percentile point of the maximum χ^2 values in 10 000 simulated case-control panels ($g(i,j)^{P=.01}$). Combinations of the numbers of mHag$^+$ (vertical coordinates) and mHag$^-$ (horizontal coordinates) samples satisfying the above condition are shown in color gradients corresponding to different max r^2 values between the target SNP and one or more nearby Phase II HapMap SNPs (r^2_{max}), ranging from 0.4 to 1.0. Calculations were made for 3 HapMap population panels, CHB + JPT (top), YRI (middle), and CEU (bottom) and for different false positive and negative rates, $f_P = f_N = 0$ (left), $f_P = 0.1, f_N \cong 0$ (middle), and $f_P = 0.1, f_N = 0.05$ (right), considering the very low false negative assays for CRAs.

sequence and initiator methionine (CCACC-ATG) and for C-terminus deletions a stop codon (TAG).

For *UGT2B17*, a series of C-terminus deletion mutants with approximately 200 bp spacing was first constructed as above. For further mapping, N-terminus deletion mutants were added to the region that was deduced to be potentially encoding the CTL-1B2 epitope. For prediction of a CTL epitope, the HLA Peptide Binding Predictions algorithm on the BioInformatics & Molecular Analysis Section (BIMAS) website (http://www.bimas.cit.nih.gov/molbio/hla_bind/)[19] was used because HLA-A*0206 has a similar binding motif to that of A*0201.

Epitope reconstitution assay

The candidate mHag epitopes and allelic counterpart peptides (in case of SLC1A5) were synthesized by standard Fmoc chemistry. ^{51}Cr-labeled mHag$^-$ donor LCL were incubated with graded concentrations of the peptides and then used as targets in standard CRAs.

Results and discussion

Statistical approach and estimation of potential overfitting

We reasoned that the mHag locus recognized by a given CTL clone could be defined by grouping LCLs from a HapMap panel into mHag$^+$ and mHag$^-$ subpanels according to their susceptibility to lysis by the CTL clone and then performing an association scan using the highly qualified HapMap data set containing more than 3 000 000 SNP markers. The relevant genetic trait here is expected to show near-complete penetrance, and the major concern with this approach arises from the risk of overfitting observed phenotypes to one or more incidental SNPs with this large number of HapMap SNPs under the relatively limited size of freedom due to small numbers of independent HapMap samples (90 for JPT + CHB and 60 for CEU and YRI, when not including their offspring).[13]

To address this problem, we first estimated the maximum sizes of the test statistics (here, χ^2 values) under the null hypothesis (ie, no associated SNPs within the HapMap set) by simulating 10 000 case-control HapMap panels under different experimental conditions, and compared them with the expected size of test statistic values from the marker SNPs associated with the target SNP, assuming different linkage disequilibrium (LD), or r^2 values in between. As shown in Figure 1, the possibility of overfitting became progressively reduced as the number of LCLs increased, which would allow for identification of the target locus in a broad range of r^2 values, except for those mHags having very low minor allele frequencies (MAF) below

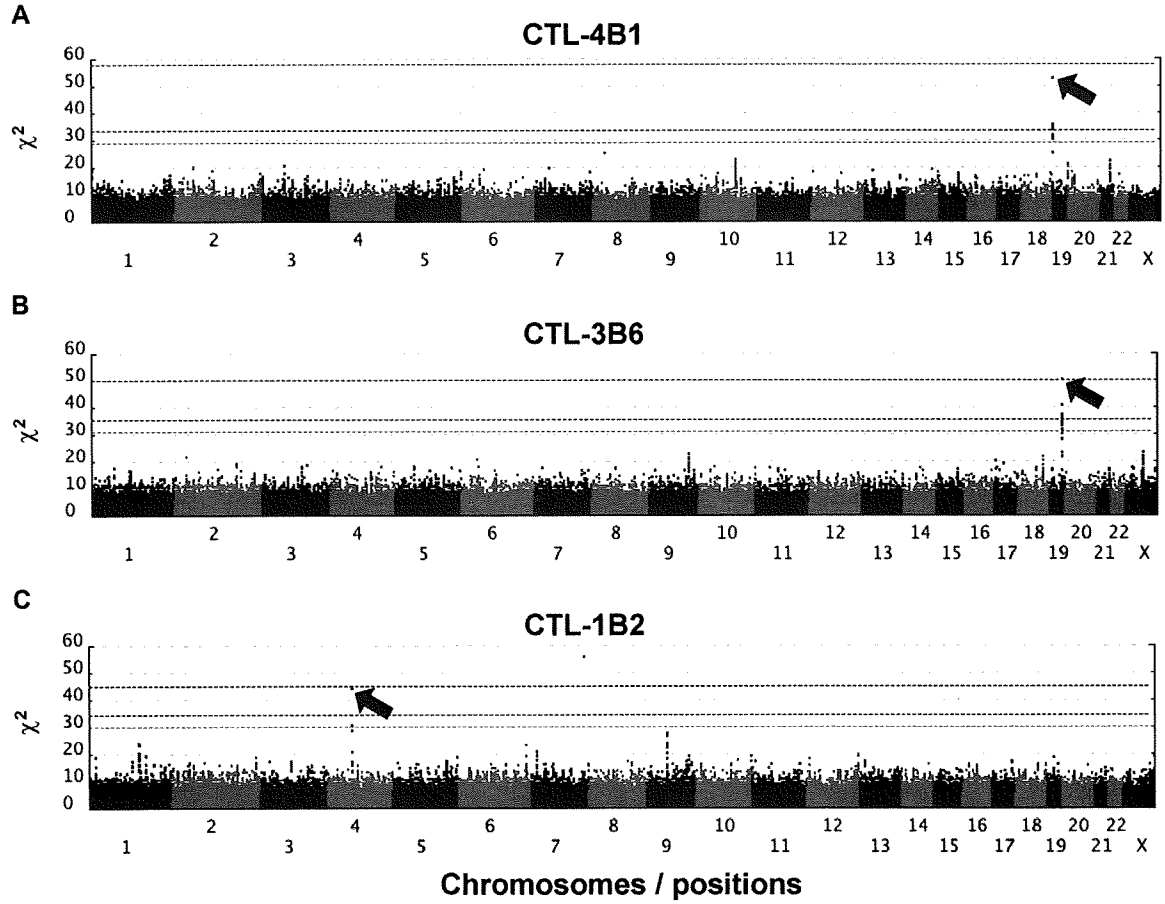

Figure 2. Genome-wide scanning to identify chromosome location of mHag. χ^2 values were plotted against positions on each chromosome for each of 3 mHags recognized by CTL-4B1 (A), CTL-3B6 (B), and CTL-1B2 (C). Chromosomes are displayed in alternating colors. Threshold χ^2 values corresponding to the genome-wide $P = 10^{-3}$ (dark blue) and 10^{-2} (light blue), as empirically determined from 100 000 random permutations, are indicated by broken lines, while the theoretically possible maximum values are shown with red broken lines. The highest χ^2 value in each experiment is indicated by a red arrow.

approximately 0.05. According to our estimation using the Phase II HapMap data (see "Methods"), the majority (> 90%) of common target SNPs (MAF > ~ 0.05) could be captured by one or more HapMap SNPs with more than 0.8 of r^2 (Figure S1, available on the *Blood* website; see the Supplemental Materials link at the top of the online article), ensuring a high probability of detecting an association (Figure 1 left panels). The simulation of pseudo-Phase II sets generated from the ENCODE regions provided a similar estimation.[13] False positive and negative immunophenotyping results could also complicate the detection, reducing the expected test statistics through the "apparent" r^2 values ($\hat{r}^2$), as defined by

$$(1) \qquad \hat{r}^2 = r^2 \times \frac{(1 - f_P - f_N)^2}{(1 - f_P + f_N q)(1 - f_N + f_P/q)}$$

where f_P, f_N, and q represent false typing probabilities with positive and negative LCL panels, and the ratio of the positive to the negative LCL number, respectively. However, the high precision of cytotoxicity assays ($f_P \sim < 0.1$, $f_N \sim = 0$) limits this drawback from the second term to within acceptable levels and allows for sensitive mHag locus mapping with practical sample sizes (Figure 1 middle and right panels), suggesting the robustness of our novel approach.

Evaluation of the detection power for known mHags

Based on these considerations, we then assessed whether this approach could be used to correctly pinpoint known mHag loci (Table S1). Because the relevant mHag alleles are common SNPs and directly genotyped in the Phase II HapMap set, or if not, located within a well-defined LD block recognized in this set (Figure S2), their loci would be expected to be uniquely determined with an acceptable number of samples, as predicted from Figure 1. To test this experimentally, we first mapped the locus for HA-1^H mHag[7] by evaluating recognition of the HLA-A*0206–transduced HapMap cell panel with HLA-A*0206–restricted CTL-4B1.[20] After screening 58 well-growing LCLs from the JPT + CHB panel with CRAs using CTL-4B1 (Figure S3A; Tables S2,S3), we obtained 37 mHag$^+$ and 21 mHag$^-$ LCLs, which were tested for association at 3 933 720 SNP loci. The SNP (rs1801284) encoding the mHag is located within a HapMap LD block on chromosome 19q13.3, but is not directly genotyped within this data set. The genome-wide scan clearly indicated a unique association with the HA-1^H locus within the *HMHA1* gene, showing a peak χ^2 statistic of 52.8 (not reached in 100 000 permutations) at rs10421359 (Figures 2A,3A; Tables S2,S3).

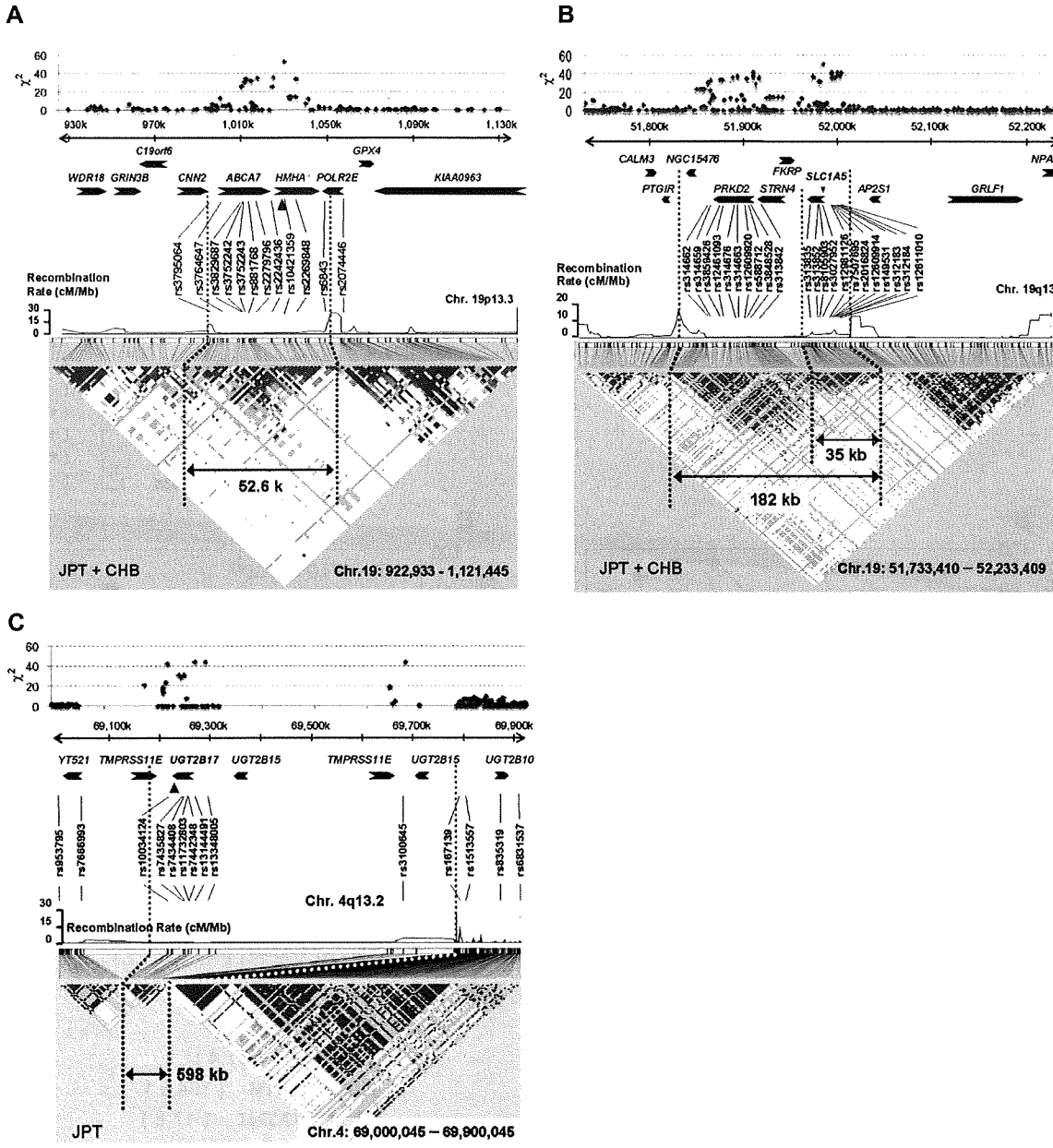

Figure 3. Regions of mHag loci identified by HapMap scanning. LD structures around the SNPs showing peak statistical values (in JPT + CHB) are presented for each mHag locus identified with (A) CTL-4B1, (B) CTL-3B6, and (C) CTL-1B2. Regional χ^2 plots are also provided on the top of each panel. LD plots in pairwise D's with recombination rates along the segment were drawn with HaploView software version 4.0 (http://www.broad.mit.edu/mpg/haploview/). The size and location of each LD block containing a mHag locus are indicated within the panels. Significant SNPs (blue letters), as well as other representative SNPs, are shown in relation to known genes. The positions of the SNPs showing the highest statistic values (red letters) are indicated by red arrowheads.

Identification of novel mHags

We next applied this method to mapping novel mHags recognized by CTL clone 3B6, which is HLA-B*4002–restricted; and CTL clone 1B2, which is HLA-A*0206–restricted. Both clones had been isolated from peripheral blood samples of post-HSCT different patients. In preliminary CRAs with the JPT + CHB panel, allele frequencies of target mHags for CTL-3B6 and CTL-1B2 in this panel were estimated as approximately 25% and approximately 45%, respectively (data not shown). After screening 72 JPT + CHB LCLs with CTL-3B6, 36 mHag$^+$ and 14 mHag$^-$ LCLs were obtained, leaving 22 LCLs undetermined based on empirically determined thresholds (> 51% for mHag + LCLs and < 11% for mHag-LCLs; Figure S3B, Tables S2,S4). As shown in Figure 2B, the χ^2 statistics calculated from the immunophenotyping data produced discrete peaks in the LCL sets. The peak in chromosome 19q13.3 for the CTL-3B6 set showed the theoretically maximum χ^2 value of 50 (not reached in 100 000 permutations) at rs3027952, which was mapped within a small LD block of

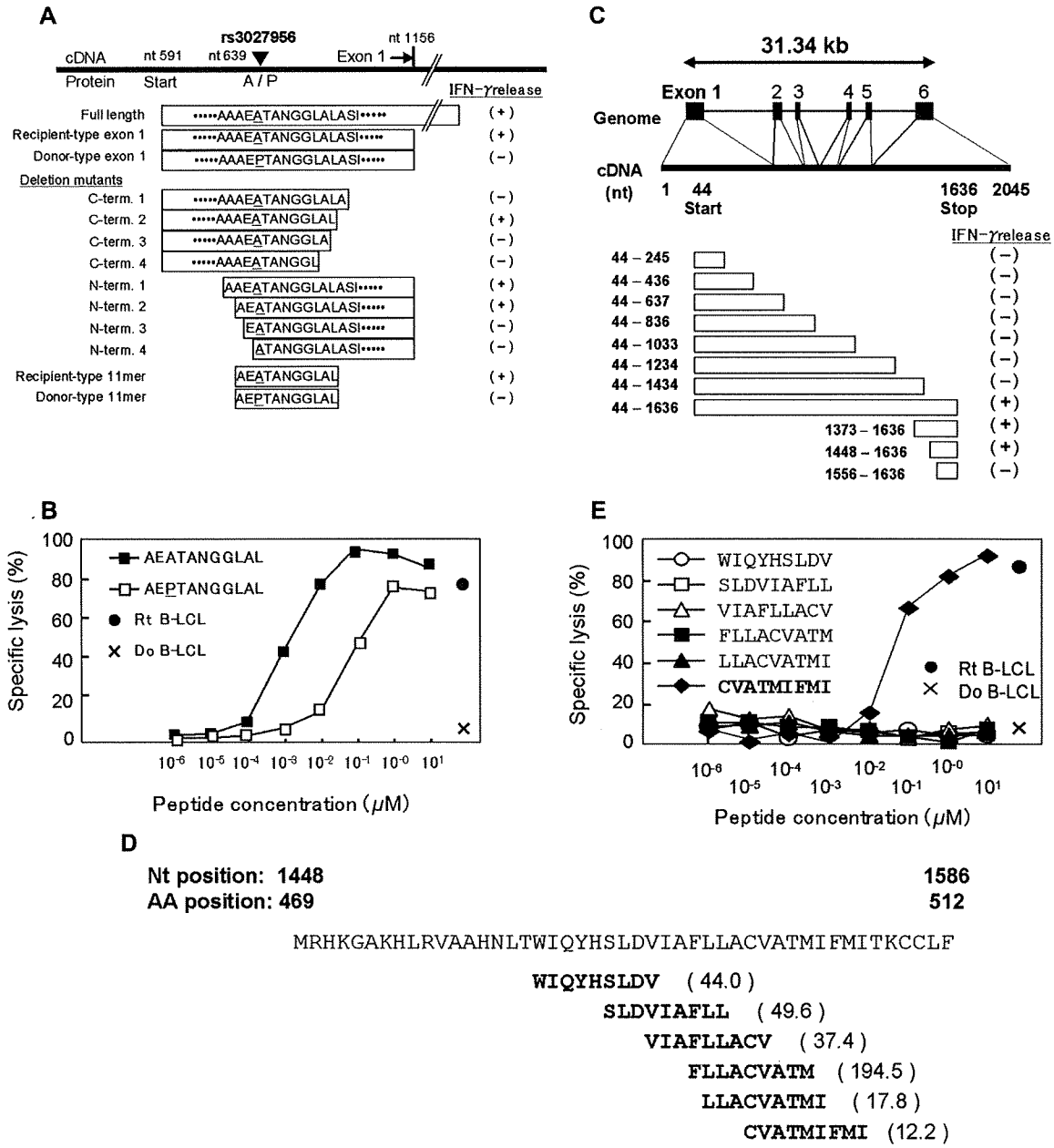

Figure 4. Epitope mapping. (A) Determination of the *SLC1A5* epitope by deletion mapping. Plasmids encoding recipient full-length *SLC1A5*, exon 1 of recipient and donor, exon 1 with various N- and C-terminus deletions around the amino acid encoded by SNP rs51983014, and minigenes encoding AEATANGGLAL and its allelic counterpart AEPTANGGLAL were constructed and transfected into HLA-B*4002–transduced 293T cells. Interferon (IFN)-γ was assessed by ELISA (right column) after coculture of CTL-3B1 with 293T transfectants. (B) Epitope reconstitution assay with synthetic undecameric peptides, AEATANGGLAL and AEPTANGGLAL. (C) Structure of the *UGT2B17* gene and screening of *UGT2B17* cDNA and deletion mutants. HLA-A*0206–transduced 293T cells were transfected with each plasmid and cocultured with CTL-2B1. IFN-γ production from CTL-1B2 (right column) indicated that the epitope was likely encoded by nucleotides 1448-1586, including 30 nucleotides from position 1566 that could potentially encode part of the epitope. (D) Epitope prediction using the HLA Peptide Binding Predictions algorithm.[19] Because HLA-A*0201 and -A*0206 have similar peptide binding motifs,[30] the algorithm for HLA-A*0201 was used to predict candidate epitopes recognized by CTL-1B2. Values in parentheses indicate the predicted half-time of dissociation. (E) Epitope reconstitution assays with graded concentrations of synthetic nonameric peptides shown in panel D.

approximately 182 kb, or more narrowly within its 35 kb sub-block containing a single gene, *SLC1A5*, as a candidate mHag gene (Figure 3B). In fact, when expressed in 293T cells with HLA-B*4002 transgene, recipient-derived, but not donor-derived, *SLC1A5* cDNA was able to stimulate IFN-γ secretion from CTL-3B6 (Figure 4A), indicating that *SLC1A5* actually encodes the target mHag recognized by CTL-3B6. Conventional epitope mapping using a series of deletion mutants of *SLC1A5* cDNA finally identified an undecameric peptide, AEATANGGLAL, as the minimal epitope (Figure 4A). The donor-type AEPTANGGLAL induced IFN-γ with a 2-log lower efficiency, suggesting that AEPTANGGLAL may not be transported efficiently into the ER

because endogenous expression of a minigene encoding AEPTANGGLAL was not recognized by CTL-3B1 (Figure 4B). Unfortunately, although the peak statistic value showed the theoretically maximum value for this data set, it did not conform to the relevant SNP for this mHag (rs3027956) due to high genotyping errors of the HapMap data at this particular SNP. However, the result of our resequencing showed complete concordance with the presence of the rs3027956 SNP and recognition in the cytotoxicity assay (Table S4).

Similarly, 13 $mHag^+$ and 32 $mHag^-$ LCLs were identified from the screening of 45 JPT LCLs from the same panel using CTL-1B2 (Figure S3C; Tables S2,S5). The χ^2 statistics calculated from the immunophenotyping data produced bimodal discrete peaks with this LCL set. The target locus for the mHag recognized by CTL-1B2 was identified at a peak (max $\chi^2 = 44$, not reached in 100 000 permutations) within a 598-kb block on chromosome 4q13.1, coinciding with the locus for a previously reported mHag, *UGT2B17*[18] (Figures 2C, 3C). In fact, our epitope mapping using *UGT2B17* cDNA deletion mutants (Figure 4C), prediction of candidate epitopes by HLA-binding algorithms[19] (Figure 4D) and epitope reconstitution assays (Figure 4E), successfully identified a novel nonameric peptide, CVATMIFMI. Of particular note, this mHag was not defined by a SNP but by a CNV (ie, a null allele[18]) that is in complete LD with the SNPs showing the maximum χ^2 value (Table S5). Transplanted T cells from donors lacking both *UGT2B17* alleles are sensitized in recipients possessing at least 1 copy of this gene.[18] Although LD between SNPs and CNVs has been reported to be less prominent,[21] this is an example where a CNV trait could be captured by a SNP-based genome-wide association study.

The recent generation of the HapMap has had a profound impact on human genetics.[13,15] In the field of medical genetics, the HapMap is a central resource for the development of theories and methods that have made well-powered, genome-wide association studies of common human diseases a reality.[22-28] The HapMap samples provide not only an invaluable reference for genetic variations within human populations, but highly qualified genotypes that enable gene-wide scanning. Here, we have demonstrated how effectively HapMap resources can be used for genetic mapping of clinically relevant human traits. No imputations and tagging strategies are required[25,28] and the potential loss of statistical power due to very limited sample sizes is circumvented by accurate immunologic detection of the traits.

Using publicly available HapMap resources, high-throughput identification of mHag genes is possible without highly specialized equipment or expensive microarrays. Except for clinically irrelevant mHags with very low allele frequencies (eg, MAF $< 5\%$), the target of a given CTL can be sensitively mapped within a mean LD block size, typically containing just a few candidate genes. The methodology described here will facilitate construction of a large panel of human mHags including those presented by MHC class II molecules, and promote our understanding of human allo-immunity and development of targeted allo-immune therapies for hematologic malignancies.[1,2] The HapMap scan approach may be useful for exploring other genetic traits or molecular targets (eg, differential responses to some stress or drugs), if they can be discriminated accurately through appropriate biologic assays. In this context, the recent report that we may reprogram the fate of terminally differentiated human cells[29] is encouraging, indicating possible exploration of genotypes that are relevant to cell types other than immortalized B cells.

Acknowledgments

We thank Drs P. Martin and W. Ho for critically reading the manuscript; and Ms Keiko Nishida, Dr Ayako Demachi-Okamura, Dr Yukiko Watanabe, Ms Hiromi Tamaki, and the staff members of the transplant centers for their generous cooperation and technical expertise.

This study was supported in part by a grant for Scientific Research on Priority Areas (B01; no.17016089) from the Ministry of Education, Culture, Science, Sports, and Technology, Japan; grants for Research on the Human Genome, Tissue Engineering Food Biotechnology and the Second and Third Team Comprehensive 10-year Strategy for Cancer Control (no. 26) from the Ministry of Health, Labor, and Welfare, Japan; and a grant-in-aid from Core Research for Evolutional Science and Technology (CREST) of Japan.

Authorship

Contribution: M.K. performed most of immunologic experiments and analyzed data and wrote the manuscript; Y.N. performed the majority of genetic analyses and analyzed the data; H.T., T.K., M.Y., S.M. and K.Tsujimura performed research; K.Taura contributed to the computational simulation; Y.I., Taro T., K.M., Y.K. and Y.M. collected clinical data and specimens; T.I., H.T., S.R.R., Toshitada T. and K.K. contributed to data analysis and interpretation, and writing of the article; and Y.A. and S.O. supervised the entire project, designed and coordinated most of the experiments in this study, and contributed to manuscript preparation.

Conflict-of-interest disclosure: The authors declare no competing financial interests.

Correspondence: Seishi Ogawa, MD, PhD, Department of Hematology and Oncology, Department of Regeneration Medicine for Hematopoiesis, The 21st Century COE Program, Graduate School of Medicine, University of Tokyo, 7-3-1, Hongo, Bunkyo-ku, Tokyo 113-8655, Japan; e-mail: sogawa-tky@umin.ac.jp; or Yoshiki Akatsuka, MD, PhD, Division of Immunology, Aichi Cancer Center Research Institute, 1-1 Kanokoden, Chikusa-ku, Nagoya 464-8681, Japan; e-mail: yakatsuk@aichi-cc.jp.

References

1. Bleakley M, Riddell SR. Molecules and mechanisms of the graft-versus-leukaemia effect. Nat Rev Cancer. 2004;4:371-380.
2. Spierings E, Goulmy E. Expanding the immunotherapeutic potential of minor histocompatibility antigens. J Clin Invest. 2005;115:3397-3400.
3. de Rijke B, van Horssen-Zoetbrood A, Beekman JM, et al. A frameshift polymorphism in P2X5 elicits an allogeneic cytotoxic T lymphocyte response associated with remission of chronic myeloid leukemia. J Clin Invest. 2005;115:3506-3516.
4. Marijt WA, Heemskerk MH, Kloosterboer FM, et al. Hematopoiesis-restricted minor histocompatibility antigens HA-1- or HA-2-specific T cells can induce complete remissions of relapsed leukemia. Proc Natl Acad Sci U S A. 2003;100:2742-2747.
5. Spierings E, Hendriks M, Absi L, et al. Phenotype frequencies of autosomal minor histocompatibility antigens display significant differences among populations. PLoS Genet. 2007;3:e103.
6. Brickner AG, Warren EH, Caldwell JA, et al. The immunogenicity of a new human minor histocompatibility antigen results from differential antigen processing. J Exp Med. 2001;193:195-206.
7. den Haan JM, Meadows LM, Wang W, et al. The minor histocompatibility antigen HA-1: a diallelic gene with a single amino acid polymorphism. Science. 1998;279:1054-1057.

8. Dolstra H, Fredrix H, Maas F, et al. A human minor histocompatibility antigen specific for B cell acute lymphoblastic leukemia. J Exp Med. 1999; 189:301-308.
9. Kawase T, Akatsuka Y, Torikai H, et al. Alternative splicing due to an intronic SNP in HMSD generates a novel minor histocompatibility antigen. Blood. 2007;110:1055-1063.
10. Akatsuka Y, Nishida T, Kondo E, et al. Identification of a polymorphic gene, BCL2A1, encoding two novel hematopoietic lineage-specific minor histocompatibility antigens. J Exp Med. 2003;197: 1489-1500.
11. Kawase T, Nanya Y, Torikai H, et al. Identification of human minor histocompatibility antigens based on genetic association with highly parallel genotyping of pooled DNA. Blood. 2008;111:3286-3294.
12. Risch N, Merikangas K. The future of genetic studies of complex human diseases. Science. 1996;273:1516-1517.
13. The International HapMap Consortium. The International HapMap Project. Nature. 2003;426:789-796.
14. The International HapMap Consortium. A second generation human haplotype map of over 3.1 million SNPs. Nature. 2007;449:851-861.
15. The International HapMap Consortium. A haplotype map of the human genome. Nature. 2005; 437:1299-1320.
16. Akatsuka Y, Goldberg TA, Kondo E, et al. Efficient cloning and expression of HLA class I cDNA in human B-lymphoblastoid cell lines. Tissue Antigens. 2002;59:502-511.
17. Riddell SR, Greenberg PD. The use of anti-CD3 and anti-CD28 monoclonal antibodies to clone and expand human antigen-specific T cells. J Immunol Methods. 1990;128:189-201.
18. Murata M, Warren EH, Riddell SR. A human minor histocompatibility antigen resulting from differential expression due to a gene deletion. J Exp Med. 2003;197:1279-1289.
19. Parker KC, Bednarek MA, Coligan JE. Scheme for ranking potential HLA-A2 binding peptides based on independent binding of individual peptide side-chains. J Immunol. 1994;152:163-175.
20. Torikai H, Akatsuka Y, Miyauchi H, et al. The HLA-A*0201-restricted minor histocompatibility antigen HA-1H peptide can also be presented by another HLA-A2 subtype, A*0206. Bone Marrow Transplant. 2007;40:165-174.
21. Redon R, Ishikawa S, Fitch KR, et al. Global variation in copy number in the human genome. Nature. 2006;444:444-454.
22. Barrett JC, Cardon LR. Evaluating coverage of genome-wide association studies. Nat Genet. 2006;38:659-662.
23. Nannya Y, Taura K, Kurokawa M, Chiba S, Ogawa S. Evaluation of genome-wide power of genetic association studies based on empirical data from the HapMap project. Hum Mol Genet. 2007;16:2494-2505.
24. Pe'er I, de Bakker PI, Maller J, Yelensky R, Altshuler D, Daly MJ. Evaluating and improving power in whole-genome association studies using fixed marker sets. Nat Genet. 2006;38:663-667.
25. Marchini J, Howie B, Myers S, McVean G, Donnelly P. A new multipoint method for genome-wide association studies by imputation of genotypes. Nat Genet. 2007;39:906-913.
26. Altshuler D, Daly M. Guilt beyond a reasonable doubt. Nat Genet. 2007;39:813-815.
27. Bowcock AM. Genomics: guilt by association. Nature. 2007;447:645-646.
28. de Bakker PI, Burtt NP, Graham RR, et al. Transferability of tag SNPs in genetic association studies in multiple populations. Nat Genet. 2006;38: 1298-1303.
29. Takahashi K, Tanabe K, Ohnuki M, et al. Induction of pluripotent stem cells from adult human fibroblasts by defined factors. Cell. 2007;131: 861-872.
30. Sudo T, Kamikawaji N, Kimura A, et al. Differences in MHC class I self peptide repertoires among HLA-A2 subtypes. J Immunol. 1995;155: 4749-4756.

Brief report

Impact of macrophage infiltration of skin lesions on survival after allogeneic stem cell transplantation: a clue to refractory graft-versus-host disease

Satoshi Nishiwaki,[1] Seitaro Terakura,[1] Masafumi Ito,[2] Tatsunori Goto,[1] Aika Seto,[1] Keisuke Watanabe,[1] Mayumi Yanagisawa,[1] Nobuhiko Imahashi,[1] Shokichi Tsukamoto,[1] Makoto Shimba,[1] Yukiyasu Ozawa,[1] and Koichi Miyamura[1]

Departments of [1]Hematology and [2]Pathology, Japanese Red Cross Nagoya First Hospital, Nagoya, Japan

We retrospectively reviewed 104 biopsy specimens of previously untreated skin acute graft-versus-host disease (GVHD) within 100 days after allogeneic stem cell transplantation, and analyzed the relationship between types of infiltrating cells and clinical outcomes. Counting the total number of $CD8^+$ T cells, $CD163^+$ macrophages, and $CD1a^+$ dendritic cells in 4 fields under original magnification ×200, the infiltration of more than 200 cells of $CD163^+$ macrophages (many macrophages [MM]) was the only significant predictor for refractory GHVD (odds ratio, 3.79; 95% confidence interval, 1.22-11.8; $P = .02$). In 46 patients given steroid treatments, MM was the only significant predictor for refractory acute GVHD (odds ratio, 5.05; 95% confidence interval, 1.19-21.3; $P = .03$). Overall survival of patients with MM was significantly lower than that of those with an infiltration of less than 200 cells of $CD163^+$ macrophages. Macrophage infiltration of skin lesions could be a significant predictive factor for refractory GVHD and a poor prognosis. (Blood. 2009;114: 3113-3116)

Introduction

Macrophages are phagocytic cells with various abilities, such as phagocytosis, antigen-presenting, and secretion of cytokines.[1,2] Recently, it was revealed in human sequential biopsy data that recipient macrophages contributed to acute graft-versus-host disease (GVHD) by antigen-presenting and secreting cytokines, causing the activation and proliferation of $CD8^+$ T cells.[3] We focused on macrophage involvement in acute GVHD, especially on the relationship between the macrophage infiltration of skin lesions and refractory GVHD.

Methods

Between January 1997 and October 2007 at the Japanese Red Cross Nagoya First Hospital, we used skin biopsy specimens within 100 days after allogeneic stem cell transplantation (allo-SCT) of skin lesions clinically considered acute GVHD without any GVHD treatment from 104 patients who underwent allo-SCTs. We analyzed the relationship between types of infiltrating cells and clinical outcomes by counting the total number of $CD8^+$ T cells, $CD163^+$ macrophages, and $CD1a^+$ dendritic cells in 4 fields of a skin biopsy specimen under original magnification ×200. Immunohistochemical analysis using paraffin sections was performed using monoclonal antibodies against CD8, CD163, and CD1a (Novocastra). CD163 is a member of the scavenger receptor cystein-rich superfamily and is an exclusive marker for macrophages, playing a major role in the scavenging components of damaged cells.[4-7]

The endpoints of this study were the outcomes of acute GVHD and overall survival (OS). Acute GVHD was diagnosed and graded according to the consensus criteria.[8] We defined refractory GVHD as that exhibited by patients who had persistent lesions after primary steroid treatments. To establish parameters, we analyzed the numbers of infiltrating $CD8^+$ T cells (≤ 100/4 fields [few T cells; FT] vs > 100/4 fields [many T cells; MT]), numbers of infiltrating $CD163^+$ macrophages (≤ 200/4 fields [few macrophages; FM] vs > 200/4 fields [many macrophages; MM]), disease risk (low vs high), human leukocyte antigen (HLA) disparity (match vs mismatch), donor source (related vs unrelated), graft source (bone marrow vs peripheral blood), age at allo-SCT (≤ 50 years vs > 50 years), conditioning regimen (conventional regimens vs reduced intensity regimens), and skin GVHD stage at biopsy (stages 1-2 vs stages 3-4). A significance level of $P < .05$ was used for all analyses, which were based on all data available as of August 31, 2008. Protocols were approved by the Japanese Red Cross Nagoya First Hospital's Institutional Review Board, and all patients provided informed consent in accordance with the Declaration of Helsinki.

Results and discussion

Table 1 summarizes the characteristics of patients and information gathered about GVHD. We divided patients into 4 groups according to the amount of infiltrating cells (FM and FT, 60.6%; MT and FM, 18.2%; MT and MM, 10.6%; and FT and MM, 10.6%). We noted a striking difference among patients in the types of infiltrating cells in skin GVHD lesions (Figure 1A). The distributions of numbers of infiltrating cells also exhibited a

Submitted March 9, 2009; accepted June 28, 2009. Prepublished online as *Blood* First Edition paper, July 30, 2009; DOI 10.1182/blood-2009-03-209635.

The publication costs of this article were defrayed in part by page charge payment. Therefore, and solely to indicate this fact, this article is hereby marked "advertisement" in accordance with 18 USC section 1734.

Table 1. Information on patient characteristics, acute GVHD, and skin biopsy

Characteristic	Value
Patient characteristics	
Total no. of patients	104
Median age at allo-SCT, y (range)	40.5 (19-61)
Male/female	65/39
Disease risk, low/high	51/53
HLA, match/mismatch	72/32
Donor, unrelated/related	67/37
Graft, BM/PB/CB	89/11/4
Conditioning, conventional/RIST	78/26
Median observation period, mo (range)	13.7 (0.7-120.7)
Acute GVHD	
Stage skin (at the time of biopsy), 1/2/3/4	22/57/25/0
Skin (the maximal severity), 1/2/3/4	16/25/52/11
Gut, 0/1/2/3/4	69/9/8/15/3
Liver, 0/1/2/3/4	82/5/3/9/5
Grade (at the time of the biopsy), I/II/III/IV	58/41/4/1
Grade (the maximal severity), I/II/III/IV	28/44/19/13
Primary steroid treatment, yes/no	46/58
Second treatment, yes/no	18/30
Outcome of GVHD, improved/refractory	84/20
Skin lesion	
Median date of appearance, days (range)	24 (5-81)
Median date of skin biopsy, days (range)	31.5 (6-82)
Median date of highest stage of skin GVHD, days (range)	34 (9-90)
No. of infiltrating $CD8^+$ cells	65 (2-305)
No. of infiltrating $CD163^+$ cells	132.5 (38-372)
No. of infiltrating $CD1a^+$ cells	7 (0-122)

Disease risk low indicates acute leukemia in first remission; CML, in first chronic phase; MDS, refractory anemia or nonmalignant hematologic disease; disease risk high, all other diagnoses; HLA match, identical HLA-A, -B, and -DRB1 loci; HLA mismatch, at least one disparity at one of these loci; BM, bone marrow; PB, peripheral blood; CB, cord blood; and RIST, reduced intensity conditioning regimens.

considerably wide variety (Figure 1B). The median number of infiltrating $CD8^+$ T cells was 65 (range, 2-305), that of infiltrating $CD163^+$ macrophages was 132.5 (range, 38-372), and thatof infiltrating $CD1a^+$ dendritic cells was 7 (range, 0-122). We used 3 skin biopsy specimens of drug rash from autologous transplantation patients as non-GVHD controls; the median numbers of $CD8^+$, $CD163^+$, and $CD1a^+$ infiltrating cells were 11 (range, 6-15), 26 (range, 19-30), and 68 (range, 65-83), respectively. MT was correlated with an HLA mismatch ($P = .047$), grade III-IV acute GVHD ($P = .03$), and MM ($P = .01$), whereas MM was correlated with unrelated donor ($P = .04$), an HLA mismatch ($P = .049$), refractory GVHD ($P = .004$), and MT ($P = .01$) using χ^2 analyses. The sensitivity and specificity of MT for refractory GVHD were 25.0% and 70.5% in all 104 patients, and 25.0% and 73.3% in 46 receiving steroids, whereas those of MM were 43.8% and 82.9%, and 43.8% and 86.7%, respectively.

In 46 patients undergoing steroid treatments, the median date of the appearance of skin lesions was 17.0 days (range, 5-54 days), whereas that of skin biopsy was 27.5 days (range, 6-63 days) and that of the highest skin stage was 32.0 days (range, 9-68 days). Treatments for GVHD were considered for GVHD patients without spontaneous regression and with progression to a higher grade, except for those in which enhanced immunosuppression would not be preferable, such as encephalopathy resulting from calcineurin inhibitor or a pathologic diagnosis of intestinal transplantation-associated microangiopathy.[9,10] The median interval from the initial clinical manifestation of GVHD to the primary treatments was 4.5 days (range, 0-97 days). The dose of prednisolone was 0.5 mg/kg in 4 patients, 1 mg/kg in 20 patients, 2 mg/kg in 19 patients, 500 mg/body in 1 patient, and 1000 mg/body in 2 patients. Only MM was identified as a negative predictive factor for refractory GVHD (Table 2). In 46 patients undergoing steroid treatments, only MM was identified as a negative predictive factor for refractory GVHD (odds ratio, 5.05; 95% confidence interval [CI], 1.19-21.3; $P = .03$).

In the Cox proportional hazard model, age more than 50 years, high risk, and MM were identified as significant risk factors by univariate analyses, with MM and high risk remaining a significant risk in a multivariate analysis (Table 3). OS rates were significantly higher in FM patients compared with those in MM (Figure 1C). Uncontrolled GVHD was the cause of 6 MM patients of 11 (54.5%) who died because of transplantation-related mortality (TRM), whereas in FM patients, 3 of 24 (12.5%) died because of uncontrolled GVHD. The causes of death for the 5 MM patients who did not die of uncontrolled GVHD were infection in 3 patients, intestinal transplantation-associated microangiopathy in 1 patient, and liver failure in 1 patient. In 46 patients who underwent steroid treatments, only MM was identified as a significant risk factor in the Cox proportional hazards model (Hazard ratio 3.25; 95% CI, 1.46-7.26; $P = .004$). OS rates were significantly higher in FM patients compared with those in MM (Figure 1D). Uncontrolled GVHD was the cause of 6 MM patients of 9 (66.7%) who died because of TRM, whereas in FM patients, 3 of 15 (20.0%) died because of uncontrolled GVHD.

Our study suggested that macrophages are involved in a specific type of acute GVHD that tended to be systemic and refractory to conventional therapies, such as corticosteroids or calcineurin inhibitors.[11-13] Differences in treatment efficacy could be explained by the difference in infiltrating cell types. Although efforts have been made at predicting refractory GVHD,[14-17] no confirmed factor has been established to date. Our findings could prove to be a relatively simple and useful method directly related to the prognosis of patients.

Macrophages could not be completely suppressed by current therapies for acute GVHD mainly targeting T cells. Considered together with

Table 2. Analyses of predictive factors for refractory GVHD in all 104 patients

Parameter	Odds ratio (95% CI)	P
More than 50 y old	1.21 (0.35-4.19)	.76
High disease risk	1.29 (0.44-3.76)	.65
Graft PB (vs BM)	1.19 (0.23-6.11)	.83
Unrelated donor	0.91 (0.30-2.73)	.86
HLA mismatch	1.96 (0.66-5.84)	.23
Conventional regimens	0.94 (0.27-3.23)	.92
Skin stage 3 or 4 at biopsy	1.97 (0.69-5.68)	.21
MT (> 100 $CD8^+$ cells)	1.26 (0.37-4.27)	.71
MM (> 200 $CD163^+$ cells)	3.79 (1.22-11.8)	.02